THE IMPACT OF THE INSTALLATION OF AN ESTUARINE DAM ON SEDIMENT DISTRIBUTION AND ACCUMULATION RATES IN THE GEUM ESTUARY, SOUTH KOREA

A Thesis

by

JOSHUA HOLLAND ALARCON

Submitted to the Office of Graduate and Professional Studies of
Texas A&M University
in partial fulfillment of the requirements for the degree of

MASTER OF MARINE RESOURCES MANAGEMENT

Chair of Committee,	Timothy Dellapenna
Committee Members,	David Retchless Peng Lin
Head of Department,	Kyeong Park

May 2021

Major Subject: Marine Resources Management

ABSTRACT

The Geum River is the third longest river in South Korea. Prior to 1994, the Geum River had an active river-mouth estuary with an upstream salt wedge. In 1994, the Geum River Dam was completed 9 km upstream from the mouth of the river within the lower estuarine portion of the river. The installation of the dam converted the system into a short tidal basin with a dramatically reduced tidal prism and an artificially modulated freshwater inflow, generally eliminating the salt wedge dynamics and reducing the tidal prism by approximately 54%. Analyses of a series of sediment vibracores, collected both upstream and downstream of the dam, was conducted for grain-size distributions as well as excess ^{210}Pb and $^{239+240}$Pu geochronologies for select cores. Analyses of seven cores reveals that there are three stages to the sedimentary history recorded in the cores: 1) pre-dam installation conditions, 2) transitional condition, which occurred after the installation of the dam during the period when the reservoir was filling with water and there was no sluice gate release of water or suspended sediment, and 3) post reservoir fill, when water and suspended sediment were released from the dam. Above the dam, coarse sediment that would have been deposited in the mouth of the estuary is instead trapped in the upper arm of the estuary, and finer sediment rapidly accumulates at the face of the dam. Below the dam, rather than coarse fluvial sediment accumulating, fine sediment rapidly accumulates due to the removal of the bedload from the post-dam sediment budget of the estuary.

ACKNOWLEDGEMENTS

I would like to thank my committee chair, Dr. Tim Dellapenna, and my committee members, Dr. David Retchless, and Dr. Peng Lin for their guidance and support throughout the course of this research.

Thank you also to my friends and colleagues and the department faculty and staff for making my time at Texas A&M University a great experience.

Finally, thank you to my family for their encouragement, support and love.

CONTRIBUTORS AND FUNDING SOURCES

Contributors

This work was supervised by a thesis committee consisting of Professor Tim Dellapenna [advisor] and Dr. David Retchless of the Department of Marine and Coastal Environmental Science and Dr. Peng Lin of the Department of Marine Sciences.

Guidance and assistance in methods was provided by Dr. Tim Dellapenna and Dr. Peng Lin. Analyses depicted in this thesis were conducted in part by Jon Rogers of the Department of Marine Science.

All other work conducted for the thesis was completed by the student independently.

Funding Sources

The field component of this study was supported by Inha University. Partial support for travel was supported by the Moody Travel Grant from Texas A&M University Galveston.

TABLE OF CONTENTS

Page

LIST OF FIGURES

Page

1. INTRODUCTION

1.1. Estuaries and Environmental Significance

Estuaries and coastlines worldwide are subject to morphological changes imposed by not only natural processes, but also anthropogenic modifications, including installation of coastal infrastructure and water control structures. Depending on the disciplinary approach, estuaries may be defined in different terms. From the geological perspective, we use the Pritchard (1967) definition that states that an estuary is "a semi-enclosed coastal body of water, which has free connection with the open sea, and within which sea water is measurably diluted with freshwater derived from land drainage". In terms of environmental management and sustainability, estuaries are among the most important coastal features for a number of reasons including locations for human development, high rates of biological productivity (Williams, Dellapenna and Lee, 2013) and essential nursery grounds for both fin and shellfish (Mukaimi et al., 2018). These environmentally sensitive ecosystems are susceptible to both natural and anthropogenic change via a variety of mechanisms, including rising sea level, subsidence, the frequency and magnitude of tropical and extratropical storms and the construction of dams or water control structures, which are installed to meet agricultural needs driven by population and economic growth (Vorosmarty et al., 2009).

The impacts on estuaries as a result of industrial and urban development include changes in shoreline configuration, fluvial discharge, tidal characteristics, sediment transport processes, and sediment dynamics cumulatively leading to extensive alteration

of these natural systems (Williams et al., 2013 and 2014). Changes in sedimentary dynamics can range from meso- and macro-scales such as tidal flats and channel morphology to mega-scale including sediment budget and changes in the volume of the tidal prism (Wang et al., 2015).

The Yeongsan estuary is a relatively deep water (average depth 15 m) macro-tidal estuary. Williams et al. (2014) discovered that within the Yeongsan estuary, after the installation of the estuarine dam, although there was little change in sediment type, the sedimentation rates increased tenfold or greater throughout much of the estuary. Previous studies including Williams et al., 2013 and 2014, Wellbrock (2020), Bartlett (2019) and others found that the installation of the estuarine dam resulted in an overall decrease in estuarine length thus causing a reduction in the tidal prism. This, in turn, can lead to a rapid sediment deposition in estuaries post-dam construction (Chang, 2020) and is the primary driver for creating the changes in both sediment rates and sediment types deposited where changes occurred. Williams et al. (2013) found that the installation of estuarine dams within the shallow, micro-tidal Nakdong estuary resulted in a tenfold increase in sedimentation rates and that areas which were formerly mud dominated became sand dominated and areas which had been sand dominated became mud dominated, collectively representing a mega-scale change to the system.

The Geum estuary, a shallow-water, macro-tidal estuary, which forms at the mouth of the Geum River, provides an excellent case study for which to compare and contrast previous investigations by Williams. The purpose of this study is to assess the impact of the installation of the Geum Estuarine Dam on the sedimentation rates and any

possible changes in sediment type which has accumulated in both the Geum estuary and proximal nearshore area of the estuary. It is hypothesized that installation of the dam has resulted in: 1) a rapid accumulation of sediment within the estuary and within the nearshore, and 2) a change in the sedimentary types as areas that had been previously mud-dominated are now accumulating sand and formerly sand-dominated areas are now accumulating mud.

2. BACKGROUND

2.1. Study Area

The Geum River is located along the central western coast of South Korea. At approximately 401 km with a drainage area of about 9828 km², the Geum River is the third longest river and has the third largest drainage basin in South Korea (Jeong et al., 2014) (Fig. 1). The upstream river-bed is comprised of coarser gravel (median grain-size ~43 mm) while the gravel becomes progressively finer moving downstream (median grain-size 17 mm) (Lee and Lee, 2020). The Geum Estuary, a semidiurnal, macrotidal system with tidal ranges from 2.8 m (neap) to 6.0 m (spring), opens into the Yellow Sea where the annual sedimentation load from the river is estimated to be around 5.6×10^6 tons (Jeong et al., 2014). The area has been subject to urbanization; this has been accompanied by a reduction in forest area within the river basin, from 65% in 1975 to 62% in 2015 (Lee and Lee, 2020).

The construction of the 1994 Geum River Estuary Dam 4.3 km upstream from the river mouth altered the system from a well-mixed estuary with a salt wedge that extended 60 km upstream to a partially-mixed estuary with a completely blocked salt wedge at the face of the dam, significantly reducing the tidal prism and altering the estuarine circulation pattern (Jeong et al., 2014) (Fig. 2). The construction of the dam prompted the formation of tidal flats and incised submarine channels on the seaward side of the dam. The installation of the dam also reduced the estuarine portion downstream (Jeong et al., 2014). The dam's sluice gates open from the top and infrequent opening of

Figure 1: Map of South Korea highlighting the Geum Estuary created using ArcMap 10.7.1.

the 20 sluice gates at ebbing tide allows for intermittent high-intensity discharge (~20 million tons of freshwater discharge per opening) from the river to flow out to the Yellow Sea (Cho et al., 2016), allowing the release of suspended load, but trapping bedload behind the dam. As a result of these hydrodynamic changes, sedimentation rates near the Geum River Estuary Dam were reported to have more than tripled (from <6 cm/yr to ~20 cm/yr) leading to a reduction in current velocity (Kim et al., 2006).

Bartlett (2019) found that construction of an estuarine dam in the Geum Estuary converted 54% of the former estuary to freshwater lake above the dam and caused a loss

of 1.2 km² of surface area above the lake. This loss of 54% of the surface area of the estuary also indicates that there was a 54% loss in the estuary's tidal prism. Wellbrock (2020) shows from 1984 to 2018 a 1.295% loss of surface-water area that occurred mostly on the river bar islands. However, Wellbrock (2020) also reported a 9.284% gain in the Geum Estuary land cover (% area coverage) as seen in the deposition on the southern tip of the former delta indicating that the flood tidal delta is actually growing in size (Fig. 3).

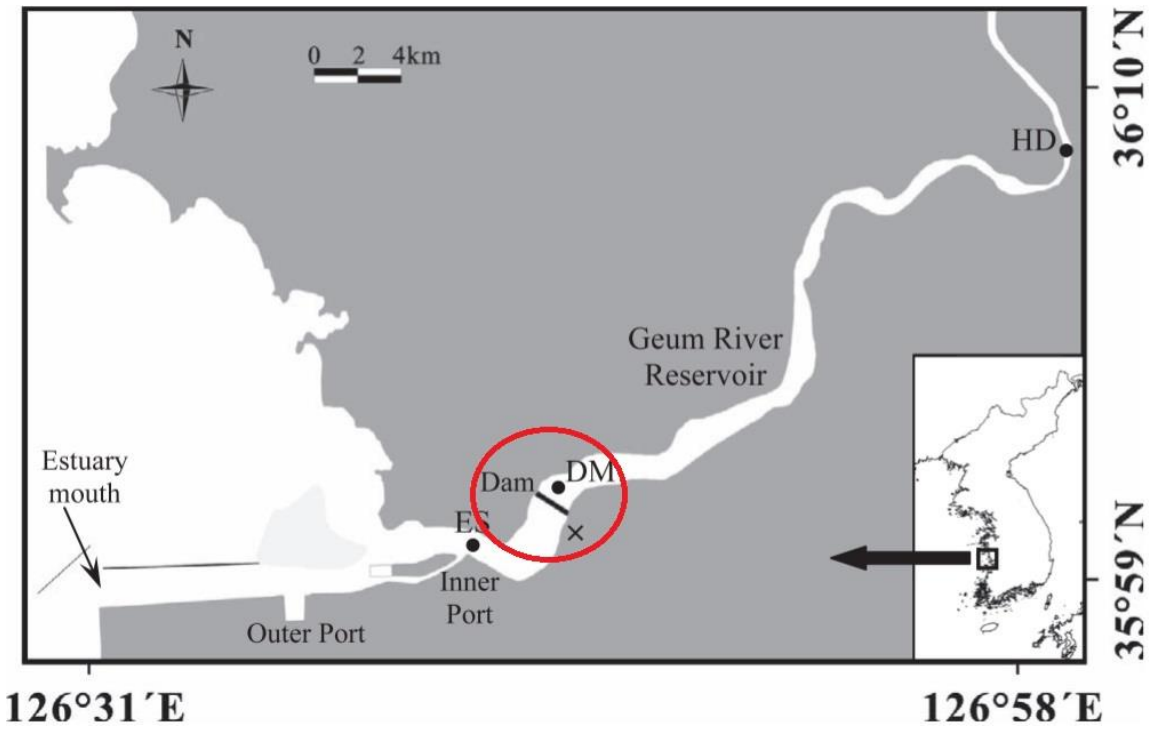

Figure 2: Drainage basin of the Geum River as depicted by Jeong et al., 2014.

2.2. Radioisotope Analysis

In the 1970's, radioisotope analyses in lacustrine (Krishnaswamy et al., 1971) and coastal (Koide et al., 1972; Chanton et al., 1983) environments became more widely-used to determine sediment accumulation rates in areas that are undergoing rapid geomorphological changes. While there is a higher degree of uncertainty of ^{137}Cs and ^{210}Pb in sandy environments due to lower radioisotope concentrations, the use of ^{210}Pb, ^{239}Pu and ^{240}Pu in estuaries and shelf environments where fine river sediment mixes with coarser marine sediment is more applicable (Pondell et al., 2015), and therefore can be used as a tool for sediment geochronology.

2.2.1. Lead-210 (^{210}Pb)

^{210}Pb is a naturally occurring radionuclide of the ^{238}U decay series and has a half-life ($t_{1/2}$) of 22.23 y (Encyclopedia of Scientific Dating Methods). Methods to ^{210}Pb based sediment dating, first proposed by Goldberg, 1963, have been subject to modification over time. While there are alternative methods for measuring ^{210}Pb in surface sediments including the Krishnaswamy et al., 1977 Beta Method outlined in Eakins and Morrison, 1977 and the Joshi, 1987 ^{210}Bi Gamma-Ray Method, trends in ^{210}Pb analysis have shown that amounts of ^{210}Pb fluctuate at the surface due to mixing, and decrease logarithmically with depth. Depending on the depth of the core and the local sedimentation rates, the nuclear fallout layer, a peak in atomic testing and activity in 1963-1964, and other facies in the core can be observed and used to determine a more precise morphology of the study area.

Figure 3: Loss of Surface Water in the Geum estuary as depicted by (modified from) Wellbrock et al., 2019.

2.2.2. Plutonium-239+240 ($^{239+240}$Pu)

Plutonium is a radioactive chemical element that can be used as a tracer to determine soil erosion rates (Alewell et al., 2014). Anthropogenic plutonium isotopes in natural ecosystems occur as a result of nuclear weapons detonation, radioactive waste

reprocessing and nuclear accidents (Lin et al., 2019). ^{239}Pu ($t_{1/2}$ = 24100 y) and ^{240}Pu ($t_{1/2}$ = 6561 y) are the two major Pu isotopes and alpha-emitting actinides originating from the nuclear weapons and nuclear power industry (Alewell et al., 2014). ^{239}Pu decays to ^{235}U via alpha emission of the Helium nucleus (Wolfer, 2000). These isotopes strongly bind to sedimentary matter, particularly natural organic matter which serves as a Pu sink in soils (Lin et al., 2017). Trends in $^{239+240}$Pu analysis demonstrated by Alewell et al., 2014 and Xu et al., 2015 have established an exponential decline law that is to be expected with increasing depth; however, cultivated or disturbed sites may demonstrate more homogenous distribution (Xu et al., 2015).

3. METHODS

A set of twenty-three cores was collected from the Geum estuary in 2015 by Dellapenna, Lee and Rogers (Fig. 4). For these cores, an x-radiograph was acquired, grain-size distributions were determined, water content analysis was conducted on each sample interval and ^{210}Pb and $^{239+240}$Pu geochronology was performed on select cores. A series of six cores from this collection, GEC 02, 05, 06, 09, 36, and 25, in conjunction with a new core, core G19 (Fig. 4), which was collected in September of 2019 by Dellapenna, Lee and Alarcon, will serve as the focus of this study. Core G19 was collected at the same location in the estuary as Roger's cores using a Vibracore with a 7.6 cm core diameter size. Core G19 was frozen immediately with dry ice and stored for several days until processing began. The core was then thawed, split in half and prepared for x-radiography, grain-size analysis, ^{210}Pb, and $^{239+240}$Pu.

3.1. Grain-size Distribution

Samples were homogenized and analyzed for grain-size distribution using a Malvern Mastersizer 2000® laser particle diffractometer. Results for grain-size profiles are depicted as a measurement of percent composition of sand, silt and clay fractions. Grain-size analysis will prove to be an important tool in determining sedimentation rates as well as provide a historical record to the morphological changes to this area.

Figure 4: Seven Stations with cores in the Geum estuary collected by Dellapenna, Lee and Rogers, 2015 and Dellapenna, Lee and Alarcon, 2019.

3.2. Lead-210 (^{210}Pb)

^{210}Pb activities are measured indirectly using the Polonium-210 (^{210}Po) method assuming secular equilibrium between ^{210}Pb and ^{210}Po. The cores are sampled at 10 cm intervals and stored in sterile plastic bags to be prepared for ^{210}Pb analysis using a modified Virginia Institute of Marine Science (VIMS) method of Hotblock Acid Digestion. Sediments are homogenized and wet-sieved at 200 μm with a minimum amount of deionized (DI) water and then dried prior to digestion. This method contains

three phases, 1. Digestion, 2. Plating and 3. Counting. The samples are spiked with ^{209}Po as a radioactive tracer and chemically separated during digestion with concentrated Hydrochloric acid (HCl) and Nitric acid (HNO_3). The samples are then plated onto silver (Ag) planchets and ^{210}Pb and ^{210}Po isotopes are counted using alpha spectroscopy with a Canberra Alpha Analyst.

3.3. Plutonium-239+240 ($^{239+240}$Pu)

$^{239+240}$Pu activities are measured indirectly using the Plutonium-242 (^{242}Pu) tracer method assuming secular equilibrium between ^{242}Pu and $^{239+240}$Pu. The cores are sampled at 10 cm and 20 cm intervals, homogenized, and stored in sterile plastic bags in preparation for $^{239+240}$Pu analysis. Methods used for $^{239+240}$Pu analysis were developed by Santschi et al., 2002 adapted from EPA method 908.0, U.S. DOE, U.S. EPA, and Yamato, 1982 and modified by Lin et al., 2017 and Xu et al., 2016. This procedure is conducted via three phases, 1. Ashing and Digestion, 2. Column separation and 3. Plating. The samples are spiked with ^{242}Pu tracer and Column separation is conducted using UTEVA columns (eichrom., UT-C50-A) converting Pu to Pu (III). Samples are then spontaneously electroplated at 0.6 Amp for 2 hours prior to counting using alpha spectroscopy with a Canberra Alpha Analyst.

Both methods used here are more suitable for finer grained sediment such as silt and clay rather than coarser grained sand as radioactivity would be undetectable in coarser grained sediments, and therefore small sections of particular cores were excluded from this analysis.

4. RESULTS

4.1. Cores GEC 02 and 05

A transect of grain-size distribution profile for select cores, extending from offshore to above the Geum Dam, is shown in Figure 5. Core GEC 02 is the most upstream and shows that within the core, the sediment is nearly uniformly sand, with a silt content of less than 5% (Fig. 5). Core GEC 05 contains two layers, an upper layer from 0 cm - 85 cm which generally contains greater than 90% sand and around 10% silt, with generally less than 1% clay. The basal 45 cm layer can be best described as a silty mud dominated layer with two prominent sand layers (Fig. 5). The mud content within both cores GEC 02 and GEC 05 are too low and too variable to warrant excess ^{210}Pb analyses as the surface to volume ratios of sand are too low for detection of the ^{210}Pb techniques used in this study.

4.2. Core GEC 06

The grain-size profile for core GEC 06 shows that the upper 100 cm of the core is composed of silt-dominated mud, with sand content generally ranging from 5% - 7%, but as high as 13.3% and as low as 4.5% (Fig. 5). Between 100 cm and the base of the core at 130 cm, the core generally contains around 15% sand, 62% silt and 22% clay. The grain-size profile shows nearly uniform size distribution from the surface down to

100 cm, with a 10% increase in sand content and around a 5% increase in both silt and clay (Fig. 5). The excess ^{210}Pb profile for core GEC 06 shows nearly uniform activities

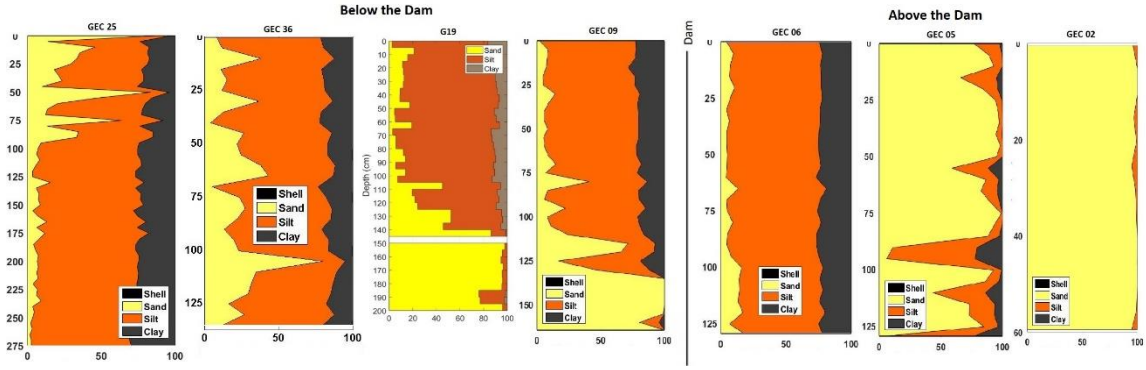

Figure 5: Sediment fractions below (GEC 25, 36, 09 and G19) and above (GEC 06, 05, and 02) the 1994 Geum Dam.

from 0 cm - 100 cm (Fig. 6). There is only one excess ^{210}Pb sample from within the 100 cm - 130 cm interval, at 115 cm, while the sample has a 50% decrease at the base of the core. Given the shift in grain-size for this interval, it is reasonable to assume that the variations in excess ^{210}Pb are heavily influenced, if not controlled by variations in grain-size and cannot be used to estimate reliable age dates. However, if it is assumed that the entire sediment column within this core was deposited post-dam installation, then this core would have an accumulation rate of 6.2 cm y^{-1}.

4.3. Cores GEC 09 and G19

Cores GEC 09 and G19 are from below the dam and were collected at approximately the same location, 0.72 miles (1163 m) apart on opposite sides of the channel (Fig. 4). The G19 core has a 105 cm surface layer dominated by silt (~75%) and clay (~20%) and a few sand stringers. From 105 cm - 140 cm, there is a transitional layer, where sand content increases down the core in a stepwise fashion, generally from 20% to 80% (Fig. 5). A basal sand layer is found from 140 cm to 200 cm at the base of the core and generally contains approximately 75% sand. Core GEC 09 grain-size distribution follows a similar trend to core G19, with surface layer down to 110 cm dominated by silt (~70%) and clay (25%) (Fig. 5). A transitional layer exists from 110 cm -135 cm, where the sand content increases from 24% sand at 110 cm to 100% sand at 135 cm, and contains a 10 cm thick sand dominated layer. A basal sand layer generally containing 100% exists from 135 cm to the base of the core at 165 cm (Fig. 5).

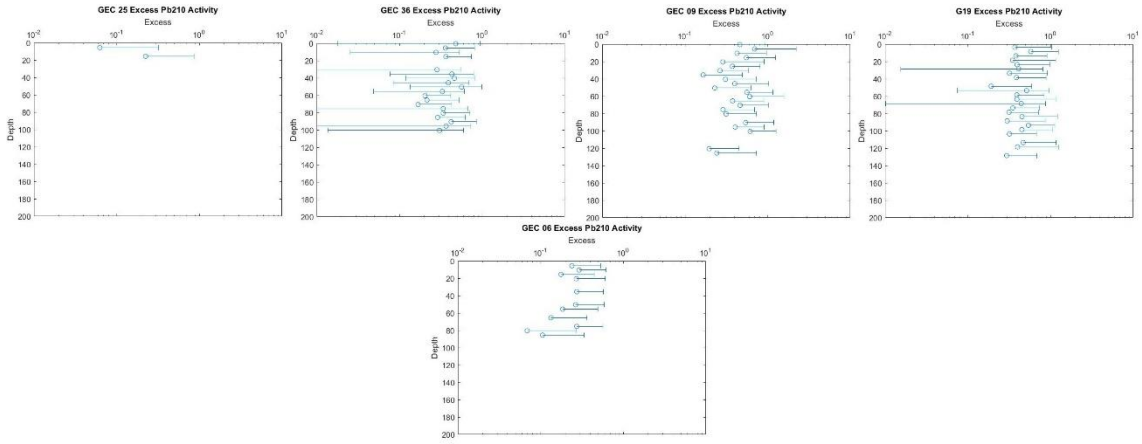

Figure 6: Excess 210Pb activity for cores below the dam (GEC 25, 36, 09 and G19) and above the dam (GEC 06).

Prior to performing ^{210}Pb analyses, the samples were wet sieved to remove the sand content. The excess ^{210}Pb profile for core GEC 09 (Fig. 6) reveals that within the surface layer (0 cm – 105 cm), the excess activity is nearly uniform, suggesting relatively rapid deposition. Within the transition interval (105 cm – 140 cm), although the sand was removed, the variability in the excess ^{210}Pb correlates strongly with the variability of the silt content. This likely results from the significant differences between the surface area to volume ratio between silt and clay rather than the decrease of excess ^{210}Pb being a function of radioisotope decay. Within the basal sand layer (140 cm – 200 cm), excess ^{210}Pb is generally below detection limits (Fig. 6). The consistent range of ^{210}Pb activity in concurrence with the uniform silt and clay layer are to be expected given this cores location in the upper estuary just below the dam where fine fluvial sediments are rapidly deposited. Assuming that the entire upper and transitional layer of

130 cm was deposited between the installation of the dam in 1994 and the collection of the core in 2015, then the accumulation rate for the post-dam sediments averages 6.19 cm y^{-1}.

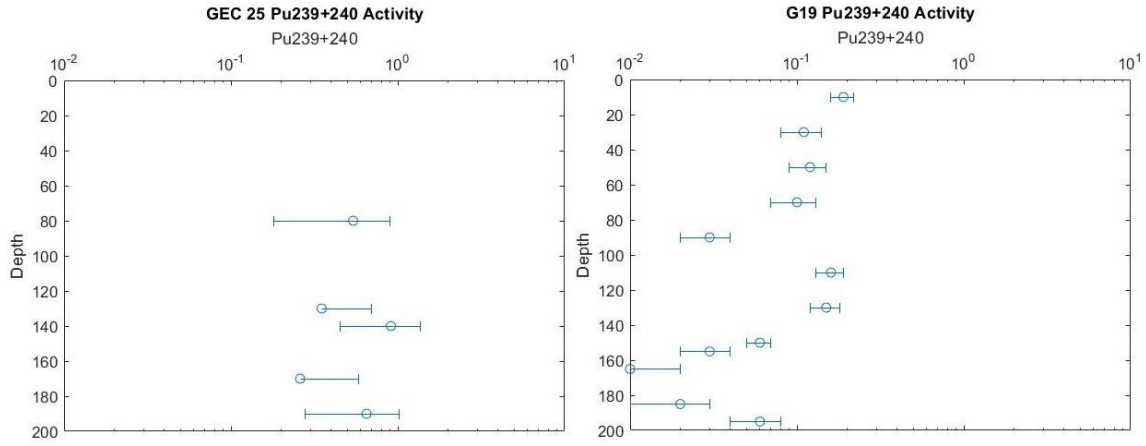

Figure 7: 239+240Pu activity for cores GEC 25 and G19.

The profile of excess ^{210}Pb activities from G19 (Fig. 6) show that within the interval from 0 cm - 120 cm, the activities are relatively uniform (fluctuating between 1.55 and 3.80 dpm g^{-1}), suggesting rapid deposition. The lower activities coincide with intervals with higher sand content. There is a steady decrease in activity from 110 cm to 140 cm (0.23 dpm g^{-1}), which coincides with the increase in sand content and decrease in mud content (Fig. 6). Since ^{210}Pb preferentially partitions to the fine grain fraction, the decrease in activity is likely the result of the decrease in the mud fraction rather than a

slower depositional rate. Below 140 cm, where there is generally less than 10% mud in the core, the excess ^{210}Pb is too low to detect. This is also likely a result of the loss of a mud fraction rather than isotopic decay.

The $^{239+240}$Pu profile for core G19 has a very coarse sample interval in comparison to the excess ^{210}Pb and grain-size profiles (Fig. 7). These analyses are substantially more expensive and time consuming, so only a limited sample run was conducted. The $^{239+240}$Pu profile within the surface interval shows a steady decrease in activity from the surface down to 90 cm. The next deepest sample is within the transitional interval and the activities are much higher. The $^{239+240}$Pu approach background levels in the upper portion of the basal sand layer, but increase to above 0.5 Bq/kg for the basal samples at 192 cm and 195 cm (Fig. 7). It should be noted that in this basal interval, there was an approximately 20% increase in silt (Fig. 5). The higher silt content appears to have had a high enough surface area to volume ratio to permit the detection of $^{239+240}$Pu. The presence of detectable $^{239+240}$Pu in these intervals confirms that these sediments in this interval were deposited after $^{239+240}$Pu was introduced into the environment, after 1963. The presence of detectable $^{239+240}$Pu at the base of the core, 50 cm below where excess ^{210}Pb is detectable in the core confirms that the decrease in excess ^{210}Pb within the transitional layer is a function of the lack of clay in the core rather than an exponential decrease in excess ^{210}Pb activity (Fig. 7). In addition, if we use 1963 as a maximum age for this 60 cm thick deposit, then we can estimate a minimum accumulation rate for sand in this layer of 1.94 cm y^{-1}. However, assuming that the entire upper and transitional layer of 140 cm was deposited between dam

installation in 1994 and core collection in 2019, then the accumulation rate for G19 for the post-dam sediments averages 5.83 cm y^{-1}.

4.4. Core GEC 36

Core GEC 36, 140 cm long, is generally mud dominated and contains a variable silt content ranging from 20% - 75%, but a nearly uniform clay content (approximately 20%) (Fig 5). It also contains a series of six layers where the sand content increases, the silt content decreases but the clay content varies little. Core GEC 36 shows relatively uniform excess ^{210}Pb activities (range of 1.164 to 3.645 dpm g-1) from 0 cm-100 cm depth suggesting rapid deposition of fine sediments (Fig 6). Once again, the impact of the variability in clay content on the shape of the ^{210}Pb profile is well defined here as ^{210}Pb preferentially partitions to the fine grain fraction. Similar to G19 and GEC 09, the decrease in activity throughout core GEC 36 is likely the result of the decrease in the mud fraction, or six sand spikes, rather than a slower depositional rate.

4.5. Core GEC 25

Core GEC 25 is from offshore and 12 km to the north of the transect. The grain-size profiles show two separate intervals in the core. The upper interval, extending from the surface to 107 cm, although mud dominated (25% - 30% clay and 20% - 60% silt), contains a series of 6 dominant sand layers, where silt content decreases but clay content varies little, and where each sand layer has progressively less sand (Fig. 5). Below this, from 107 cm to the base of the core, the core consists nearly uniformly of less than 10%

sand, 68% silt and approximately 25% clay, with a slight, but steady decrease in sand content with depth where there was only 2.5% sand at the base of the core (Fig. 5). The excess ^{210}Pb activity profile for core GEC 25 reveals that within the surface interval, there is a step-wise decrease in excess ^{210}Pb down to the base of the surface interval, with lower excess ^{210}Pb activities within the sand layer. The excess ^{210}Pb activity, beginning with the 110 cm sample interval, abruptly decreases to below 0.01 dpm g-1, indicating that the excess activities have reached background levels (Fig. 6). The $^{239+240}$Pu profile also reveals that below 110 cm, $^{239+240}$Pu activities are non-detectable (Fig. 7). Taken together, the data suggest that there has been an active recent deposition from the surface of the core to 110 cm. Below 110 cm, the lack of detectable $^{239+240}$Pu suggests that the sediment in this interval was deposited before 1963, and the lack of excess ^{210}Pb suggests further that this sediment is older than 5 half-lives of ^{210}Pb (~100 years). If we assume that all of the sediment that has accumulated above 110 cm was deposited since 1994, when the dam was opened, then there is an accumulation rate at this site of 5.24 cm y^{-1}.

5. DISCUSSION

5.1. Below the Dam System Changes

As stated previously, the Geum River is the third longest river with the third largest drainage basin in South Korea. Prior to the installation of the Geum 1994 dam, the mouth of the Geum River, dominated by sand, would have behaved like a delta during periods of high discharge with a seaward salt wedge and rapid accumulation of sand, and reverted back to an estuary during low discharge periods with a salt wedge farther upstream. Therefore, the accumulation of mud, pre-dam installation, likely occurred offshore within a subaqueous delta while the accumulation of sand occurred within the mouth of the estuary. This can be observed in Fig. 3A, which shows an aerial image of the pre-dam river mouth, presenting a geometry consistent with a tide-dominated river delta. Aspects of this are further revealed by the presence of dominant sand layers at the base of cores G19 and GEC 09, which contain detectable $^{239+240}$Pu at the base of the core, 60 cm below the top of this basal sand layer, indicating active/rapid accumulation of approximately 2 cm y^{-1}.

The 1994 Geum Dam was designed so that the gates open from the top, mostly releasing fine-grained suspended load, mud, in the water column rather than coarser-grained sand which is trapped in the bedload. In other words, intermittent opening the dam's sluice gates will not flush coarse sediment out, but instead would release suspended material into the estuary mouth to accumulate atop previous delta sand

deposits. Below the dam, the GEC 09 and G19 post-dam strata within the estuary are mud dominated and have accumulation rates of 6 cm y^{-1}.

As a consequence of the sluice gates opening from the top, the bedload from the river has been completely removed from the post-dam sediment budget of the estuary. In the downstream direction, within the post-dam estuarine deposit, between cores GEC 36 and GEC 09, there is between a 10% and 20% increase in sand content within the sand layers (Fig. 8). This suggests an increase seaward in marine derived sand, which is consistent with the formation of a flood-tide deposit at the mouth of the estuary and a lack of river derived sand deposition within the upper reaches of the estuary. The transitional layer found in GEC 09 and G19 found directly above the pre-dam surface, where mud content increases upwards, was likely formed during the period of time just after the dam was completed, but prior to the reservoir reaching full capacity. At this time, there is little to no release of water, resulting in a much lower suspended load (i.e. mud) being deposited while sand was transported in by incoming tides.

The core GEC 25 location is 12 km north of the mouth of the Geum River, but within the coastal embayment that contains the mouth of the river. The core GEC 25 is also located 7 km offshore of the tidal flats, towards the mouth of the embayment (Fig. 4). The basal mud layer for this core is composed of relict mud likely over a century old, indicating the pre-dam site was either erosional or at least non-depositional. The accumulation of 107 cm in the 21 years between dam installation and core collection indicates that the post-dam sediment accumulated at an average rate of 5.23 cm y^{-1}.

Additionally, there is a general trend within the post-dam layer of an increase in sand content within the sand stringers found within the core.

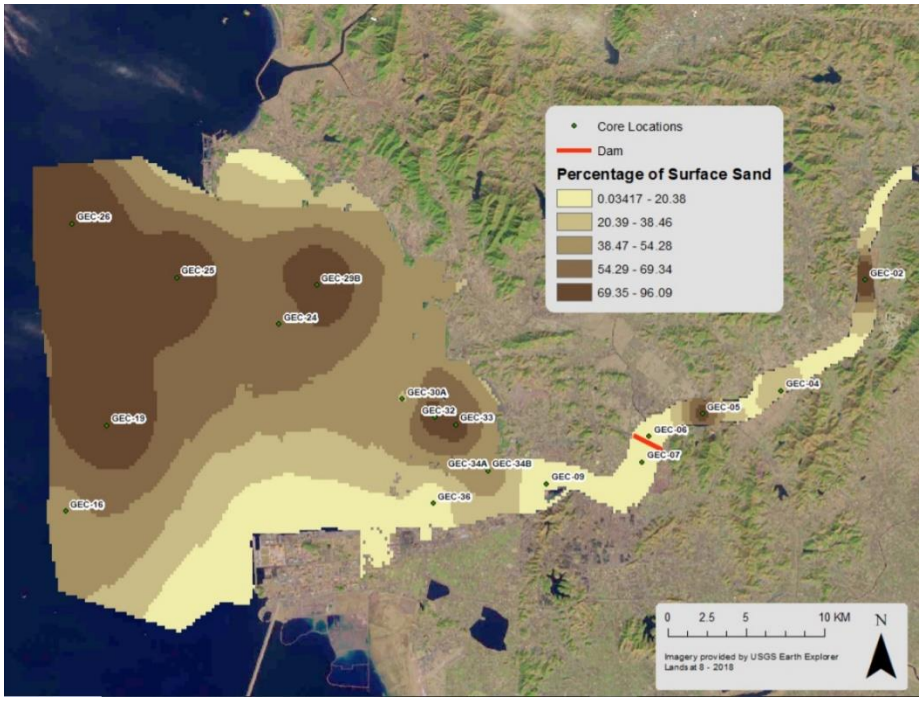

Figure 8: Percentage of Surface Sand.

The Geum estuary is similar to the Nakdong estuary in that prior to the installation of the estuarine dam, the system was a tide-dominated river mouth delta (Williams et al., 2013). The main difference between these systems is that the Nakdong is a microtidal estuary with an average tidal range of 1 m and the Geum is macrotidal

with a tidal range varying between 2.6 m - 6 m. Williams et al. (2013) found that within the Nakdong estuary, after the installation of the dam, the tidal prism had been drastically reduced and resulted in centimeters per year of mud accumulation just below the dam. Observations of the post-dam estuarine deposit suggests that, like the Nakdong estuary, that the dramatic reduction in the tidal prism in the Geum Estuary has also resulted in over a half of a decimeter per year sediment accumulation.

5.2. Above the Dam System Changes

Figure 3A shows two sand bars at the location of core GEC 06, suggesting that prior to the installation of the dam, the location of core GEC 06 was sand-dominated. This is consistent with the location being within the mouth of a river-dominated estuary prior to dam construction. Core GEC 06 was collected 400 m upstream of the dam and 483 m to the north northwest of the flood gates. The grain-size profile for GEC 06 shows that the core is composed of silt dominated mud, with an abrupt 10% increase in sand content for the basal 30 cm of the 130 cm long core (Fig. 5). The excess ^{210}Pb profile has nearly uniform activities for the upper 100 cm of the core (Fig. 6), suggesting, in addition to very rapid accumulation rates, the 50% decrease in excess activities at the base of the core likely results from the decrease in silt and clay content in the basal layer rather than isotopic decay. It is likely that the basal layer represents the earliest phase of reservoir fill just after the completion of the dam and that the upper 100 cm of mud represents a more steady-state condition. It would appear that the base of the

post-dam layer was not reached in this core, but a minimum sediment accumulation of 6.2 cm y^{-1} is estimated.

The basal 45 cm of core GEC 05, located 3.9 km upstream of the dam (Fig. 4), consists of a mud layer with two thick sand interbeds while the upper 85 cm of the core is generally sand dominated with a few muddy interbeds (Fig. 5). Core GEC 02, collected approximately 17.3 km above the dam, is the most upstream core collected in this study (Fig. 4). The core contains 95% sand or higher throughout (Fig. 5). Both the upper 85 cm of core GEC 05 and the entirety of core GEC 02 indicate that, post-dam installation, this portion of the Geum Lake is accumulating bedload sand. The lower 45 cm of GEC 05, likely a transitional layer, as well as the basal 30 cm in core GEC 06 (Fig. 5) were formed directly after dam completion, when both bed load and suspended load were trapped above the dam prior to filling of the reservoir with water. Once the reservoir had filled to capacity and the sluice gates were opened, much of the suspended load was then released into the estuary.

5.3. Overall Observations of Sedimentation Patterns in the Geum Estuary

Prior to the installation of the Geum estuarine dam, the lower Geum Estuary was a tide-dominated delta with sand accumulating along the entire river channel at rates that were on the order of 2 cm y^{-1}. After the installation of the estuarine dam, there was a short transitional period which occurred after closing of the dam but prior to the filling of the reservoir (Fig. 9). As noted in cores GEC 06 and 05 above the dam, both bedload, sand, and suspended load, mud, were accumulating. From the location of core GEC 05

to at least the location of core GEC 02, approximately 13.5 km upstream, bedload sand accumulated. After the reservoir filled, from core GEC 05 to at least GEC 02, nearly all deposition was in the form of suspended load. Just above the dam and to the north northwest, at the location of core GEC 06 (Fig. 9), primarily suspended sediment was deposited at an estimated minimum rate of 6.2 cm y^{-1}.

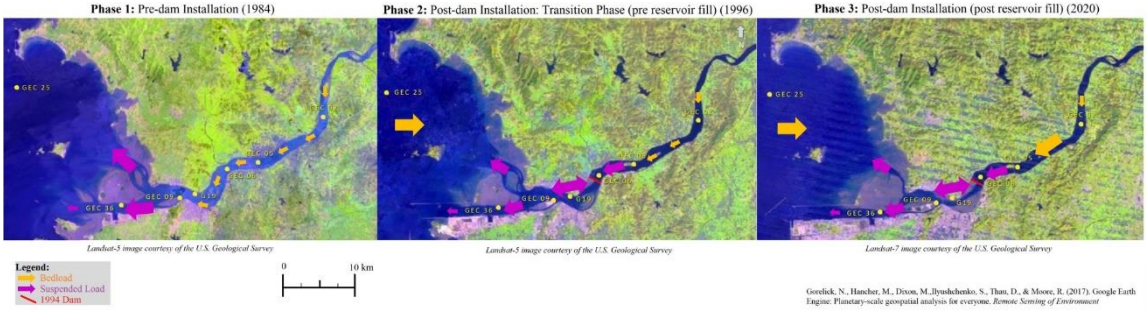

Figure 9: Three Phases of the Geum Estuary as a result of Dam Installation.

Below the dam, after the dam was installed, the bedload was cut off to the estuary. After the reservoir filled, a high suspended sediment load was sporadically released from the sluice gates and transported to the estuary and proximal nearshore (Fig. 9). Because the tidal prism has been drastically reduced within the estuary, suspended sediment is transported into the estuary when the sluice gates are not open and there is little tidal flushing to remove it, and therefore it becomes trapped. Core

GEC 25 shows that this location, a nearshore environment, has shifted from a non-depositional site with a mud bottom to a sandier site with an accumulation rate of 5.24 cm y^{-1}. The higher sedimentation coupled with the deposition of a higher sand content at this location suggests that within the inner-shelf just north of the Geum estuary, the reduction of the tidal prism allowed an area that was non-depositional to transform into and an area with extremely high sedimentation rates. Within the Nakdong estuary, in the 82 years between the installation of the first dam in 1930 and the research conducted by Williams et al. (2013), the system evolved from a funnel-shaped, tide-dominated delta/estuary to a wave-dominated estuary with new barrier islands forming offshore across the mouth of the estuary. In the case of the Nakdong, there is only a 1 m tidal range, while the Geum estuary tidal range can be as high as 7.5 m. As a result, the loss of the tidal prism within the Geum estuary means a loss of a much greater hydrodynamic forcing than the Nakdong estuary. The presence of deposit within the inner-shelf that is sand-dominated, depositing at a rate of 5.24 cm y^{-1}, suggests that the system is rapidly transforming towards a wave-dominated end-member. At the rate sediment is accumulating, this system may also become transformed into a wave-dominated estuary with barrier islands within the next century.

6. CONCLUSIONS

6.1. Research Approach and Broader Impacts

The Geum River is the third longest river in South Korea. Prior to the installation of the Geum Estuarine Dam in 1994, the mouth of the Geum River modulated between a tide-dominated delta during the high discharge periods, normally found during the summer and fall monsoon season, and a tide-dominated estuary during the dryer months between the monsoon seasons. The installation of the Geum River dam in 1994 removed 1.2 km of estuary and reduced the tidal prism by 54%. Subsequently, this has modified the delivery of fluvial sediment to the estuary, completely removing the bedload, retaining it above the dam, and modulating the discharge of suspended load to only periods when water was released from the sluice gate, which opens from the top of the dam.

Analyses of seven cores reveals that there are three stages to the sedimentary history recorded in the cores: 1) pre-dam installation conditions, 2) transitional condition, which occurred after the installation of the dam during the period when the reservoir was filling with water and there was no sluice gate release of water or suspended sediment, and 3) post reservoir fill, when water and suspended sediment were released from the dam. Above the dam, coarse sediment that would have been deposited in the mouth of the estuary is instead trapped in the upper arm of the estuary, and finer sediment rapidly accumulates at the face of the dam. Below the dam, rather than coarse

fluvial sediment accumulating, fine sediment rapidly accumulates due to the removal of the bedload from the post-dam sediment budget of the estuary.

The disturbance of natural sediment fluxes has resulted in a reduction of estuarine habitat or a loss of surface area as demonstrated by Bartlett (2019) and Wellbrock (2020). Regardless, the accumulation rates in the Geum Estuary have dramatically increased as a direct result of the installation of the 1994 Geum River Dam. In addition, this has prompted changes in sedimentary types being deposited at locations throughout the former active river delta. Estuaries worldwide are susceptible to environmental and anthropogenic change via a variety of mechanisms and the impacts imposed on estuaries as a result of industrial and urban development cause extensive alteration of these systems. Therefore, understanding the mechanics and physical processes occurring in these systems becomes vital in any attempt to preserve or restore an ecological system.

7. REFERENCES

Alewell, Christine, et al. "Suitability of 239+ 240Pu and 137Cs as tracers for soil erosion assessment in mountain grasslands." *Chemosphere* 103 (2014): 274-280.

Appleby, P. G., and F. Oldfieldz. "The assessment of 210 Pb data from sites with varying sediment accumulation rates." *Hydrobiologia* 103.1 (1983): 29-35.

Appleby, P. G., et al. "210 Pb dating by low background gamma counting." *Hydrobiologia* 143.1 (1986): 21-27.

Appleby, Peter G., and Frank Oldfield. "The calculation of lead-210 dates assuming a constant rate of supply of unsupported 210Pb to the sediment." *Catena* 5.1 (1978): 1-8.

Bartlett, Victoria Lee. “Have land use changes and Anthropogenic Modification of Estuaries resulted in changes in estuarine convergence in South Korea?” Diss. 2019.

Baskaran, M. "A search for the seasonal variability on the depositional fluxes of 7Be and 210Pb." *Journal of Geophysical Research: Atmospheres* 100.D2 (1995): 2833-2840.

Binford, Michael W. "Calculation and uncertainty analysis of 210 Pb dates for PIRLA project lake sediment cores." *Journal of Paleolimnology* 3.3 (1990): 253-267.

Chang, Jongwi, et al. "Sediment transport mechanisms in altered depositional environments of the Anthropocene Nakdong Estuary: A numerical modeling study." *Marine Geology* 430 (2020): 106364.

Chanton, Jeffrey P., Christopher S. Martens, and George W. Kipphut. "Lead-210 sediment geochronology in a changing coastal environment." *Geochimica et Cosmochimica Acta* 47.10 (1983): 1791-1804.

Cho, Jaegab, Yongsik Song, and Tae In Kim. "Numerical modeling of estuarine circulation in the Geum River Estuary, Korea." *Procedia Engineering* 154 (2016): 982-989.

Eakins, JD and, and R. T. Morrison. "A new procedure for the determination of lead-210 in lake and marine sediments." *The International Journal of Applied Radiation and Isotopes* 29.9-10 (1978): 531-536.

Encyclopedia of Scientific Dating Methods; DOI 10.1007/978-94-007-6326-5_236-1# Springer Science+Business Media Dordrecht 2014

Jeong, Yong Hoon, Jae Sam Yang, and Kyeong Park. "Changes in water quality after the construction of an estuary dam in the geum river estuary dam system, korea." *Journal of Coastal Research* 30.6 (2014): 1278-1286.

Joshi, S. "Nondestructive determination of lead-210 and radium-226 in sediments by direct photon analysis." *Journal of Radioanalytical and Nuclear Chemistry* 116.1 (1987): 169-182.

Kim, Ki-Cheol, et al. "Variations of physical oceanographic environment caused by opening and closing the floodgate in Nakdong Estuary." *Journal of the Korean Society for Marine Environment & Energy* 2.2 (1999): 49-59.

Kim, T. I., B. H. Choi, and S. W. Lee. "Hydrodynamics and sedimentation induced by large-scale coastal developments in the Keum River Estuary, Korea." *Estuarine, Coastal and Shelf Science* 68.3-4 (2006): 515-528.

Kim, Ji-Myong, et al. "Cost of Climate Change: Risk of Building Loss from Typhoon in South Korea." *Sustainability* 12.17 (2020): 7107.

Koide, Minoru, Andrew Soutar, and Edward D. Goldberg. "Marine geochronology with210Pb." *Earth and Planetary Science Letters* 14.3 (1972): 442-446.

Krishnaswamy, S., et al. "Geochronology of lake sediments." *Earth and Planetary Science Letters* 11.1-5 (1971): 407-414.

Lee, Sahong, and Jung Lyul Lee. "Estimation of Background Erosion Rate at Janghang Beach due to the Construction of Geum Estuary Tidal Barrier in Korea." *Journal of Marine Science and Engineering* 8.8 (2020): 551.

Lin, Peng, et al. "Plutonium partitioning behavior to humic acids from widely varying soils is related to carboxyl-containing organic compounds." *Environmental Science & Technology* 51.20 (2017): 11742-11751.

Lin, Peng, et al. "Nagasaki sediments reveal that long-term fate of plutonium is controlled by select organic matter moieties." *Science of The Total Environment* 678 (2019): 409-418.

Al Mukaimi, Mohammad E., et al. "Centennial record of anthropogenic impacts in Galveston Bay: Evidence from trace metals (Hg, Pb, Ni, Zn) and lignin oxidation products." *Environmental pollution* 237 (2018): 887-899.

Pondell, Christina R., et al. "Application of Plutonium Isotopes to the Sediment Geochronology of Coarse-Grained Sediments from Englebright Lake, California (USA)." *Aquatic geochemistry* 22.2 (2016): 97-115.

Pritchard, Donald W. "What is an estuary: physical viewpoint." American Association for the Advancement of Science, 1967.

Sanchez-Cabeza, J. A., P. Masqué, and I. Ani-Ragolta. "210Pb and210Po analysis in sediments and soils by microwave acid digestion." *Journal of Radioanalytical and Nuclear Chemistry* 227.1-2 (1998): 19-22.

Tims, S. G., et al. "Plutonium as a tracer of soil and sediment movement in the Herbert River, Australia." *Nuclear Instruments and Methods in Physics Research Section B: Beam Interactions with Materials and Atoms* 268.7-8 (2010): 1150-1154.

Vörösmarty, Charles J., et al. "Battling to save the world's river deltas." *Bulletin of the Atomic Scientists* 65.2 (2009): 31-43.

Wang, Z. B., et al. "Human impacts on morphodynamic thresholds in estuarine systems." *Continental Shelf Research* 111 (2015): 174-183.

Wellbrock, Nicholas Brett. “Development of a Geospatial Process for the Analysis of changes in the coastal, embayed, and estuarine surface waters of South Korea” Diss. 2020

Williams, Joshua, et al. "Mechanism for sediment convergence in the anthropogenically altered microtidal Nakdong Estuary, South Korea." *Marine Geology* 369 (2015): 79-90.

Williams, Joshua, et al. "Sedimentary impacts of anthropogenic alterations on the Yeongsan Estuary, South Korea." *Marine Geology* 357 (2014): 256-271.

Williams, Joshua R., Timothy M. Dellapenna, and Guan-hong Lee. "Shifts in depositional environments as a natural response to anthropogenic alterations: Nakdong Estuary, South Korea." *Marine Geology* 343 (2013): 47-61.

Xu, Yihong, et al. "Plutonium as a tracer for soil erosion assessment in northeast China." *Science of the Total Environment* 511 (2015): 176-185.

Xu, Chen, et al. "Role of natural organic matter on iodine and 239,240 Pu distribution and mobility in environmental samples from the northwestern Fukushima Prefecture, Japan." *Journal of environmental radioactivity* 153 (2016): 156-166.